Eur. Phys. J. Plus (2023) 138:708
https://doi.org/10.1140/epjp/s13360-023-04288-4

THE EUROPEAN PHYSICAL JOURNAL PLUS

Regular Article

Wave–wave interaction of an extended evolution equation with complete Coriolis parameters

Na Cao, XiaoJun Yin[a], LiYang Xu, ShuTing Bai

College of Science, Inner Mongolia Agriculture University, Hohhot 010018, China

Received: 2 August 2022 / Accepted: 15 July 2023

Abstract An extended evolution equation is studied by means of Hirota bilinear method in this article, and it is gained from local Cartesian coordinate system of the basic equation group by applying scaling analysis and perturbation expansions. Firstly, the equation is transformed into Hirota form by variable transformation. Secondly, based on Hirota equation, we obtained the soliton, breather, rogue wave and interaction solutions of the equation. At last, figures of these solutions and the interaction of wave–wave are showed by choosing appropriate parameters. The effects of the horizontal Coriolis parameter on the soliton, breather, rogue wave, interaction solutions are conducted. We believe that the results have significant impaction in ocean dynamics.

1 Introduction

Studied here, we focus on the Eq. (3) in reference [1], which is a mesoscale ocean model that takes into account complete Coriolis parameters, other factors such as dissipation, topography, adiabatic heating are not considered. In this document, the mass conservation equation and the momentum equation can be written as follows:

$$\begin{cases} \frac{\partial \alpha}{\partial t}+\alpha\frac{\partial \alpha}{\partial x}+\beta\frac{\partial \alpha}{\partial y}+\gamma\frac{\partial \alpha}{\partial z}=-\frac{1}{d_0}\frac{\partial p}{\partial x}+f\beta-f'\gamma, \\ \frac{\partial \beta}{\partial t}+\alpha\frac{\partial \beta}{\partial x}+\beta\frac{\partial \beta}{\partial y}+\gamma\frac{\partial \beta}{\partial z}=-\frac{1}{d_0}\frac{\partial p}{\partial y}-f\alpha, \\ \frac{\partial \gamma}{\partial t}+\alpha\frac{\partial \gamma}{\partial x}+\beta\frac{\partial \gamma}{\partial y}+\gamma\frac{\partial \gamma}{\partial z}=-\frac{1}{d_0}\frac{\partial p}{\partial z}+g\frac{\psi}{\psi_0}+f'\alpha, \\ \frac{\partial \psi}{\partial t}+\alpha\frac{\partial \psi}{\partial x}+\beta\frac{\partial \psi}{\partial y}+\gamma\frac{\mathrm{d}\psi_0}{\mathrm{d}z}=0, \\ \frac{\partial (d_0\alpha)}{\partial x}+\frac{\partial (d_0\beta)}{\partial y}+\frac{\partial (d_0\gamma)}{\partial z}=0, \end{cases} \tag{1}$$

where x is the zonal coordinate, and α is the zonal velocity; y is the meridional coordinate, and β is the meridional velocity; z is the vertical coordinate, and γ is the vertical velocity. In the whole ambient flow field, d_0 represents density and ψ_0 represents potential temperature, respectively, they are functions of z, and the temperature stratification is expressed as $\frac{\mathrm{d}\psi_0}{\mathrm{d}z}$. ψ represents the perturbation of temperature. The symbol f, f', respectively, denote the vertical component and horizontal component. The physical meanings of other symbols are in the literature [1]. An extended KdV equation is gained as model to evolve equatorial near-inertial waves via perturbation expansions and the multiple scale method, as follows:

$$C\frac{\partial A}{\partial T}+C_1\frac{\partial A}{\partial \xi}+C_2A\frac{\partial A}{\partial \xi}+C_3\frac{\partial^3 A}{\partial \xi^3}=0. \tag{2}$$

where $C=-\iint\limits_{y,z}\frac{\tilde{q}_0^*}{\overline{v}_x-c}\big(L_3(\tilde{t}_0)+L_4(\tilde{v}_{x0})\big)\mathrm{d}y\mathrm{d}z$,

$$C_1=\gamma\iint\limits_{y,z}\frac{\tilde{q}_0^*}{\overline{v}_x-c}L_2(\tilde{v}_{x0}))\mathrm{d}y\mathrm{d}z,$$

$$C_2=-\iint\limits_{y,z}\frac{\tilde{q}_0^*}{\overline{v}_x-c}\left\{L_3\left[\frac{1}{d_s}\left(\tilde{v}_{x0}\tilde{t}_0+\tilde{v}_{y0}\frac{\partial \tilde{t}_0}{\partial y}\right)\right]+L_4\left[\frac{1}{d_s}\left(\tilde{v}_{x0}^2+\tilde{v}_{y0}\frac{\partial \tilde{v}_{x0}}{\partial y}+\tilde{v}_{z0}\frac{\partial \tilde{v}_{x0}}{\partial z}\right)\right]\right\}\mathrm{d}y\mathrm{d}z,$$

$$C_3=-\iint\limits_{y,z}\frac{\tilde{q}_0^*}{\overline{v}_x-c}L_1\big[(\overline{v}_x-c)\tilde{v}_{y0}\big]\mathrm{d}y\mathrm{d}z.$$

[a] e-mail: yinxiaojun_2002@163.com (corresponding author)

Published online: 13 August 2023

Equation (2) can be reduced to:

$$\frac{\partial F}{\partial T}+a_1F\frac{\partial F}{\partial \xi}+a_2\frac{\partial^3 F}{\partial \xi^3}+a_3\frac{\partial F}{\partial \xi}=0. \tag{3}$$

where $a_1=\frac{C_2}{C}, a_2=\frac{C_3}{C}, a_3=\frac{C_1}{C}$. One key coefficient a_3 represents the horizontal component of Coriolis parameters, a_3 took effect by controlling the velocity feature of the near-inertial waves. In the reference [1], the Eq. (3) was solved by applying Jacobian elliptic function expansions; periodic and soliton solutions are obtained. Apparently, we need more meaningful exact solutions which are not available; the horizontal Coriolis parameter effects on solitons, breathers, rogue wave and interactions have not discussed.

Actually, exact solutions of nonlinear equations have an important role in many fields, like mechanics [2], plasma physics [3, 4], optics [5], acoustics [6], thermodynamics [7]. Many researchers have studied on the exact solutions of the nonlinear equations, counting in solitons [8–11], breathers [12–19], and rouge [20–22]. Breathers are local wave solutions with period, non-mediocre properties caused by collision reaction of breathers, so breathers are often used to explain the modulation instability and the generation of rouge waves [23]. Rouge solution is one of rational function solution with local characteristics of space–time; it shows up in a short period, large amplitude, extremely destructive. It suddenly appears and disappears, and the crest is extremely steep, posing a great threat to ships in the sea [24]. Many researchers also focus on interaction solutions between soliton and other solutions [25–29]. To explain some physical phenomena further, we need to construct interaction solutions among nonlinear waves.

There have many ways to get the exact solutions of nonlinear extended equations, for instance, the Hirota bilinear method [30–35], inverse scattering transformation [36–38], symbolic computation approach [39–41], Lie group method [42–44], Darboux transformation [45–47], Bäcklund transformation [48–50], and so on. The Hirota bilinear transformation uses small parameter perturbation method, and the solution of a series expansion is substituted into the bilinear equation, then compare the coefficients of the parameters in the equation to the same power, so we can get the specific expressions of the one-soliton, muti-solitons of the original equation, and the general expressions for the N-soliton can be obtained by mathematical induction. The Hirota bilinear transformation uses bilinear derivatives as a tool, and this tool has one on one relationship to the equation that is being solved. It is easy to calculate and has solved a large number of nonlinear partial differential equations effectively [51].

This paper mainly studied following points: Firstly, Hirota bilinear equation of the extended equation is obtained. Secondly, the N-soliton solutions are gained by using small parameter perturbation, breather, rogue wave, and interaction between one-soliton and one-breather, interaction between two-soliton and one-rogue that are found by using the symbolic calculation method; the solution images are given with the help of Mathematica software. Lastly, it can be found that the Rossby waves rotate clockwise with the Coriolis parameter a_3 increasing. when the wave is periodic, the period decreases with the increasing of the horizontal Coriolis parameters a_3. When studying the interaction, we found that a change in a_3 does not cause a change in the moment of the interaction.

2 The Hirota bilinear form

Under the following variable transformation:

$$u=2(\ln F)_{\xi\xi}. \tag{4}$$

where $u=u(\xi,T)$, $F=F(\xi,T)$, and $a_1=6a_2$.

Substituting (4) into (3), the Eq. (3) is transformed into the below Hirota bilinear form:

$$(D_\xi D_T+a_2D_\xi^4+a_3D_\xi^2)F\cdot F=0. \tag{5}$$

Then, there:

$$\begin{aligned}
&D_\xi D_T F\cdot F=2(F_{\xi T}F-F_\xi F_T),\\
&D_\xi^4 F\cdot F=2(F_{\xi\xi\xi\xi}F-4F_\xi F_{\xi\xi\xi}+3F_{\xi\xi}^2),\\
&D_\xi^2 F\cdot F=2(F_{\xi\xi}F-F_\xi^2).
\end{aligned} \tag{6}$$

3 The soliton solutions

Next, we follow the steps of the Hirota bilinear method to get the N-soliton solution of Eq. (3), substituting (6) into (5), we get:

$$(F_{\xi T}F-F_\xi F_T)+a_2(F_{\xi\xi\xi\xi}F-4F_\xi F_{\xi\xi\xi}+3F_{\xi\xi}^2)+a_3(F_{\xi\xi}F-F_\xi^2)=0. \tag{7}$$

Using bilinear form and small parameter perturbation method suppose:

$$F=1+\varepsilon F_1+\varepsilon^2F_2+\varepsilon^3F_3+\varepsilon^4F_4\cdots. \tag{8}$$

substituting (8) into (7) and compare the coefficients of the same power of ε to obtain a system of linear differential equations:

$$\varepsilon: \left(\partial\xi\partial T + a_2\partial^4\xi + a_3\partial^2\xi\right)F_1 = 0, \tag{9.1}$$

$$\varepsilon^2: 2\left(\partial\xi\partial T + a_2\partial^4\xi + a_3\partial^2\xi\right)F_2 = -\left(D_\xi D_T + a_2 D_\xi^4 + a_3 D_\xi^2\right)F_1\cdot F_1, \tag{9.2}$$

$$\varepsilon^3: 2\left(\partial\xi\partial T + a_2\partial^4\xi + a_3\partial^2\xi\right)F_3 = -2\left(D_\xi D_T + a_2 D_\xi^4 + a_3 D_\xi^2\right)F_1\cdot F_2, \tag{9.3}$$

$$\varepsilon^4: 2\left(\partial\xi\partial T + a_2\partial^4\xi + a_3\partial^2\xi\right)F_4 = -\left(D_\xi D_T + a_2 D_\xi^4 + a_3 D_\xi^2\right)(2F_1\cdot F_3 + F_2\cdot F_2), \tag{9.4}$$

3.1 The one-soliton solution

To solve one-soliton, we suppose:

$$F = 1 + \varepsilon F_1, F_1 = \mathrm{e}^{\theta_1}, \theta_1 = \lambda_1\xi + \omega_1 T + \theta_1^0. \tag{10}$$

With λ_1, ω_1 and θ_1^0 are arbitrary constants.
Then

$$F = 1 + \varepsilon\mathrm{e}^{\lambda_1\xi+\omega_1 T+\theta_1^0}. \tag{11}$$

Substituting (10) into (9.1), we can obtain the following equation:

$$\lambda_1\omega_1 + a_2\lambda_1^4 + a_3\lambda_1^2 = 0. \tag{12}$$

We can get:

$$\omega_1 = -(a_2\lambda_1^3 + a_3\lambda_1). \tag{13}$$

Let $\varepsilon = 1$ lead to:

$$F = 1 + \mathrm{e}^{\lambda_1\xi-(a_2\gamma_1^3+a_3\gamma_1)T+\theta_1^0}. \tag{14}$$

and we can get one-soliton solution:

$$u = 2\left[\ln\left(1 + \mathrm{e}^{\lambda_1\xi-(a_2\gamma_1^3+a_3\gamma_1)T+\theta_1^0}\right)\right]_{\xi\xi}. \tag{15}$$

3.2 The two-soliton solution

To solve two-soliton, we suppose:

$$F = 1 + \varepsilon F_1 + \varepsilon^2 F_2, F_1 = \mathrm{e}^{\theta_1} + \mathrm{e}^{\theta_2}, F_2 = \mathrm{e}^{\theta_1+\theta_2+A_{12}}. \tag{16}$$

where $\theta_i = \lambda_i\xi + \omega_i T + \theta_i^0\,(i = 1, 2)$ with λ_i, ω_i,and θ_i^0 are arbitrary constants.Then,

$$F = 1 + \varepsilon\left(\mathrm{e}^{\lambda_1\xi+\omega_1 T+\theta_1^0} + \mathrm{e}^{\lambda_2\xi+\omega_2 T+\theta_2^0}\right) + \varepsilon^2\mathrm{e}^{\lambda_1\xi+\omega_1 T+\theta_1^0+\lambda_2\xi+\omega_2 T+\theta_2^0+A_{12}}. \tag{17}$$

substituting (16) into (9.1), we can obtain the following equation:

$$\left(\lambda_1\omega_1\mathrm{e}^{\theta_1} + \lambda_2\omega_2\mathrm{e}^{\theta_2}\right) + a_2\left(\lambda_1^4\mathrm{e}^{\theta_1} + \lambda_2^4\mathrm{e}^{\theta_2}\right) + a_3\left(\lambda_1^2\mathrm{e}^{\theta_1} + \lambda_2^2\mathrm{e}^{\theta_2}\right) = 0. \tag{18}$$

we can get:

$$\omega_i = -(a_2\lambda_i^3 + a_3\lambda_i)\,(i = 1, 2). \tag{19}$$

substituting (16) into (9.2),$\mathrm{e}^{A_{12}}$ can be calculated by using Mathematica:

$$\mathrm{e}^{A_{12}} = -\frac{(\lambda_1-\lambda_2)((\omega_1-\omega_2) + a_2(\lambda_1-\lambda_2)^3 + a_3(\lambda_1-\lambda_2))}{(\lambda_1+\lambda_2)((\omega_1+\omega_2) + a_2(\lambda_1+\lambda_2)^3 + a_3(\lambda_1+\lambda_2))} \tag{20}$$

let $\varepsilon = 1$ lead to:

$$F = 1 + \mathrm{e}^{\theta_1} + \mathrm{e}^{\theta_2} - \frac{(\lambda_1-\lambda_2)((\omega_1-\omega_2) + a_2(\lambda_1-\lambda_2)^3 + a_3(\lambda_1-\lambda_2))}{(\lambda_1+\lambda_2)((\omega_1+\omega_2) + a_2(\lambda_1+\lambda_2)^3 + a_3(\lambda_1+\lambda_2))}\mathrm{e}^{\theta_1+\theta_2}. \tag{21}$$

where ω_i satisfies (19). Substituting (21) into (4), we can get two-soliton:

$$u = 2\left[\ln\left(1 + \mathrm{e}^{\theta_1} + \mathrm{e}^{\theta_2} + \mathrm{e}^{\theta_1+\theta_2+A_{12}}\right)\right]_{\xi\xi}. \tag{22}$$

where $\theta_i = \lambda_i\xi + \omega_i T + \theta_i^0\,(i = 1, 2)$, $\omega_i = -(a_2\lambda_i^3 + a_3\lambda_i)\,(i = 1, 2)$ and

$$\mathrm{e}^{A_{12}} = -\frac{(\lambda_1-\lambda_2)((\omega_1-\omega_2) + a_2(\lambda_1-\lambda_2)^3 + a_3(\lambda_1-\lambda_2))}{(\lambda_1+\lambda_2)((\omega_1+\omega_2) + a_2(\lambda_1+\lambda_2)^3 + a_3(\lambda_1+\lambda_2))}.$$

3.3 The three-soliton solution

To solve three-soliton, we suppose:

$$F = 1 + \varepsilon F_1 + \varepsilon^2 F_2 + \varepsilon^3 F_3, \tag{23}$$

$$F_1 = e^{\theta_1} + e^{\theta_2} + e^{\theta_3}, \tag{24}$$

$$F_2 = e^{\theta_1+\theta_2+A_{12}} + e^{\theta_1+\theta_3+A_{13}} + e^{\theta_2+\theta_3+A_{23}}, \tag{25}$$

$$F_3 = e^{\theta_1+\theta_2+\theta_3+A_{123}}. \tag{26}$$

where $\theta_i = \lambda_i \xi + \omega_i T + \theta_i^0\, (i = 1, 2, 3)$. Substituting (24) into (9.1), we can obtain:

$$\omega_i = -(a_2\lambda_i^3 + a_3\lambda_i)\,(i = 1, 2, 3). \tag{27}$$

substituting (24) and (25) into (9.2), $e^{A_{ij}}$ can be calculated by using Mathematica:

$$e^{A_{ij}} = -\frac{(\lambda_i - \lambda_j)((\omega_i - \omega_j) + a_2(\lambda_i - \lambda_j)^3 + a_3(\lambda_i - \lambda_j))}{(\lambda_i + \lambda_j)((\omega_i + \omega_j) + a_2(\lambda_i + \lambda_j)^3 + a_3(\lambda_i + \lambda_j))}\,(i = 1, 2, 3, i < j). \tag{28}$$

substituting (24), (25) and (26) into (9.3), F_3 can be calculated by using Mathematica:

$$F_3 = e^{\theta_1+\theta_2+\theta_3+A_{123}}. \tag{29}$$

where $e^{A_{123}} = e^{A_{12}} e^{A_{13}} e^{A_{23}}$, let $\varepsilon = 1$ lead to

$$F = 1 + e^{\theta_1} + e^{\theta_2} + e^{\theta_3} + e^{\theta_1+\theta_2+A_{12}} + e^{\theta_1+\theta_3+A_{13}} + e^{\theta_2+\theta_3+A_{23}} + e^{\theta_1+\theta_2+\theta_3+A_{123}}. \tag{30}$$

substituting (30) into (4), we can get three-soliton solution:

$$u = 2[\ln F]_{\xi\xi}. \tag{31}$$

where F satisfies formula (30). Substituting (24), (25) and (26) into (9.4), we can obtain $F_4 = 0$, so the three-soliton solution must exist, and the N-soliton solution must exist.

3.4 The N-soliton solution

The same can be obtained the N-soliton. The function F has the below formula:

$$F = \sum_{\mu=0,1} e^{\sum\limits_{i=1}^{N}\mu_i\theta_i + \sum\limits_{1\le i<j}\mu_i\mu_j A_{ij}}. \tag{32}$$

where $\theta_i = \lambda_i \xi + \omega_i T + \theta_i^0\, (i = 1, 2, 3 \cdots N)$, ω_i satisfies (27) $(i = 1, 2, 3 \cdots N)$ and $e^{A_{ij}}$ satisfies (28) $(i = 1, 2, 3 \cdots N$, $1 \le i < j)$, with λ_i,and θ_i^0 are arbitrary constants. $\sum \mu = 0, 1$ covers the sum of all possible combinations of θ_i, $\theta_j = 0, 1\, i$, $j = 1, 2, 3 \cdots N$. Putting (32) into (4), we can get N-soliton solution:

$$u = 2\left[\ln\left(\sum_{\mu=0,1} e^{\sum\limits_{i=1}^{N}\mu_i\theta_i + \sum\limits_{1\le i<j}\mu_i\mu_j A_{ij}}\right)\right]_{\xi\xi}. \tag{33}$$

where $\theta_i = \lambda_i \xi + \omega_i T + \theta_i^0 (i = 1, 2, 3 \cdots N)$,$\omega_i$ satisfies (27) $(i = 1, 2, 3 \cdots N)$ and $e^{A_{ij}}$ satisfies (28) $(i = 1, 2, 3 \cdots N$, $1 \le i < j)$.

The Fig. 1 By choosing proper parameters for (15), the dynamic diagrams of one-soliton can be described: $\lambda_1 = 1/2$, $a_2 = 1$, (a1) $a_3 = 1/8$; (a2) $a_3 = 1$; (a3) $a_3 = 2$. From Figures (a1), (a2) and (a3), the same values of λ_1 and a_2, along with a_3 increasing, the direction of wave propagation changes clockwise. Not only that, from the Figure (a4), the wave width of one-soliton solutions decreases, and the wave propagation frequency accelerates with the Coriolis parameter a_3 increasing, but Rossby waves amplitude does not change. From Figures (a5) illustrate, one-soliton has general traveling wave properties.

The Fig. 2 By choosing proper parameters for (22), the dynamic diagrams of two-soliton can be described: $\lambda_1 = 1$, $\lambda_2 = 3/2$, $a_2 = 1$, (a6) $a_3 = -2$; (a7)$a_3 = -1$; (a8) $a_3 = 7/6$. From (a6), (a7) and (a8), the same values of λ_1, λ_2 and a_2, along with a_3 increasing, the direction of wave propagation changes clockwise; at same time, the angle gradually decreases. we can clearly see that the two solitons are bright, and the collisions are elastic. Their speeds and shapes keep no change after collision; two solitons get phase shifts after the interactions, and as a_3 changes, the position of the interaction between solitons does not change. From (a9), (a10) and (a11), different values a_3 leads to the big change of density when the two waves collide. From Figures (a12), when

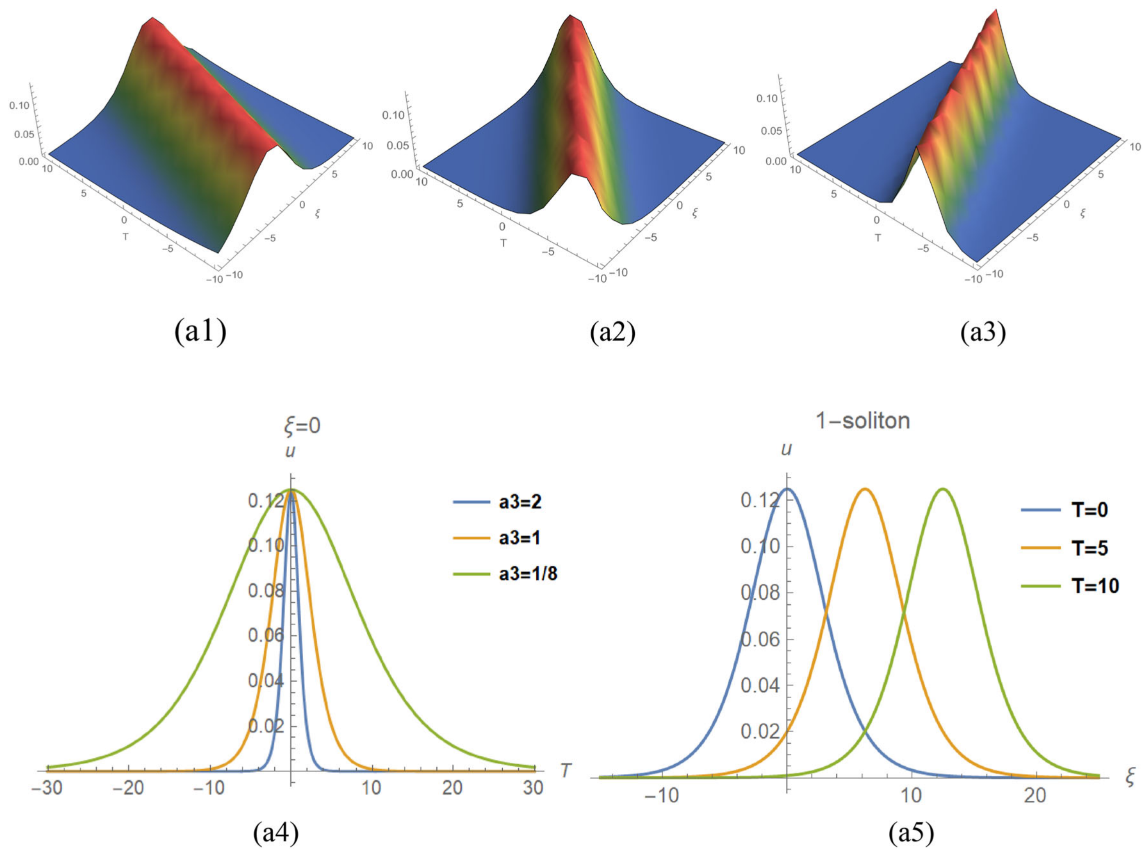

Fig. 1 One-soliton solutions of Eq. (3). Up row: 3D graphs of one-soliton solutions with $\lambda_1 = 1/2$, $a_2 = 1$ (a1) $a_3 = 1/8$; (a2) $a_3 = 1$; (a3) $a_3 = 2$. Down row: The left one is the visual diagram of a_3 transformation. The right one is the propagation of solitons overtime with $a_3 = 1$

$a_3 = -1$, we can see that the shape and amplitude of the waves change with the changing of T. The two solitons take interaction completely when $T = 0$, the amplitude goes down, which reflects the energy dissipation caused by the interaction of the two solitons. When $T = -5$ and $T = 5$, there are two axisymmetric graphs. From Figure (a13), when $\xi = 0$, the shapes of the waves are very similar, the wave width decreases, and the wave propagation frequency accelerates along a_3 increasing; Rossby waves amplitude does not change. From Figure (a14), when $T = 1$, the wave keeps its shape and shifts to the left along a_3 changing.

In Fig. 3, by choosing proper parameters for (31), the dynamic diagrams of three-soliton can be described: $\lambda_1 = 2$, $\lambda_2 = 3$, $\lambda_3 = 3/2$, $a_2 = 1$, (a15) $a_3 = -4$; (a16)$a_3 = -2$; (a17) $a_3 = 1$. From (a15), (a16) and (a17), the same values of λ_1, λ_2, λ_3 and a_2, along with a_3 increasing, the direction of wave propagation changes clockwise; at same time, the intersection angle of the three waves changes. we can see that the three solutions are bright solitons, and the collisions are elastic. Their speeds and shapes keep no change after collision; three solitons have phase shifts after the interactions, and as a_3 changes, the position of the interaction between solitons does not change. From (a18), (a19) and (a20), different values of the horizontal Coriolis parameter a_3 lead to the large change of contour density when the three waves collide. From Figures (a21), when $a_3 = -2$, we can see that the shape and amplitude of the waves change with the changing of T. The three solitons take interaction completely when $T = 0$, amplitude of waves reaches the maximum value, which reflects the energy accumulation caused by the interaction of the three solitons. From Figure (a22), when $\xi = 0$, the shapes of the waves are very similar, the wave width decreases, and the wave propagation frequency accelerates along a_3 increasing; Rossby waves amplitude does not change. From Figure (a23), when $T = 1$, the wave keeps its shape and shifts to the left along a_3 changing.

4 The one-breather wave solution

Supporting by the symbolic computation approach, the one-breather wave solution of Eq. (3) is gained, suppose:

$$f = \mathrm{e}^{-\theta_1} + c_2\mathrm{e}^{\theta_1} + c_1 \cos\theta_2, \tag{34}$$

where $\theta_1 = \lambda_1(\xi - w_1 T)$, $\theta_2 = \lambda_2(\xi + w_2 T)$, where λ_1, w_1, λ_2, w_2 are real constant.

Substituting (34) into (7) and setting the coefficients of $e^{\theta_1}\cos\theta_2$, $e^{-\theta_1}\cos\theta_2$, .

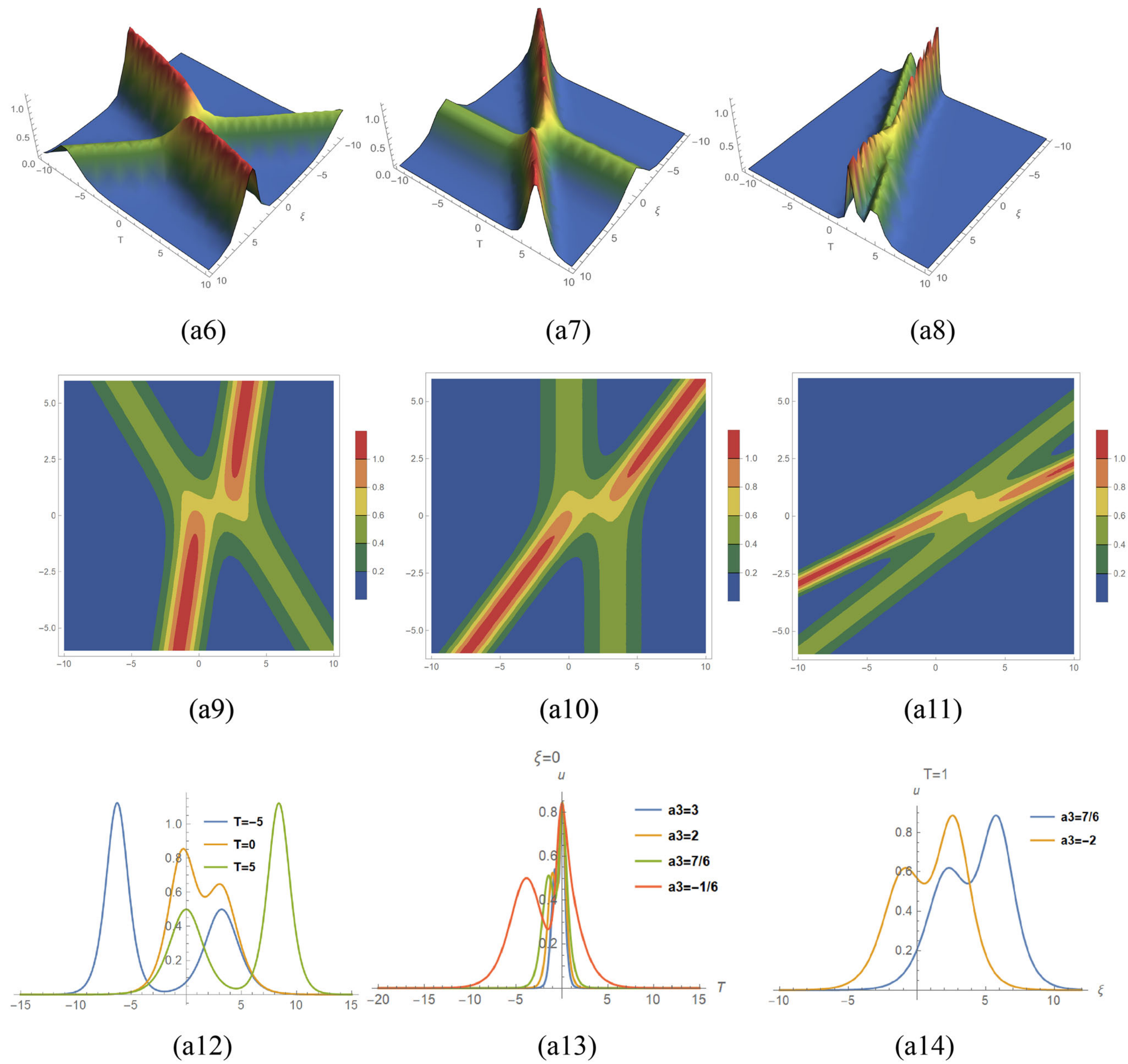

Fig. 2 Two-soliton solutions of Eq. (3). First row: 3D graphs of two-soliton solutions with $\lambda_1 = 1$, $\lambda_2 = 3/2$, $a_2 = 1$, (a6) $a_3 = -2$; (a7) $a_3 = -1$; (a8) $a_3 = 7/6$. Second row is the contour plots. Third row: 2D graphs of two-soliton solutions

$e^{\theta_1} \sin\theta_2$, $e^{-\theta_1} \sin\theta_2$ and constant term equal to zero, we get equation group as below:

$$\begin{cases} c_2\lambda_1^2(a_3 - w_1 + 4a_2\lambda_1^2) = 0, \\ -c_1\lambda_1^2(w_1 + w_2 + 4a_2\lambda_1^2) = 0, \\ -c_1c_2\lambda_1^2(w_1 + w_2 + 4a_2\lambda_1^2) = 0, \\ c_1\lambda_1^2(-2a_3 + w_1 - w_2) = 0, \\ c_1c_2\lambda_1^2(2a_3 - w_1 + w_2) = 0. \end{cases} \tag{35}$$

We select one of the solutions to continue analysis:

$$w_1 = a_3, w_2 = -a_3, a_2 = 0. \tag{36}$$

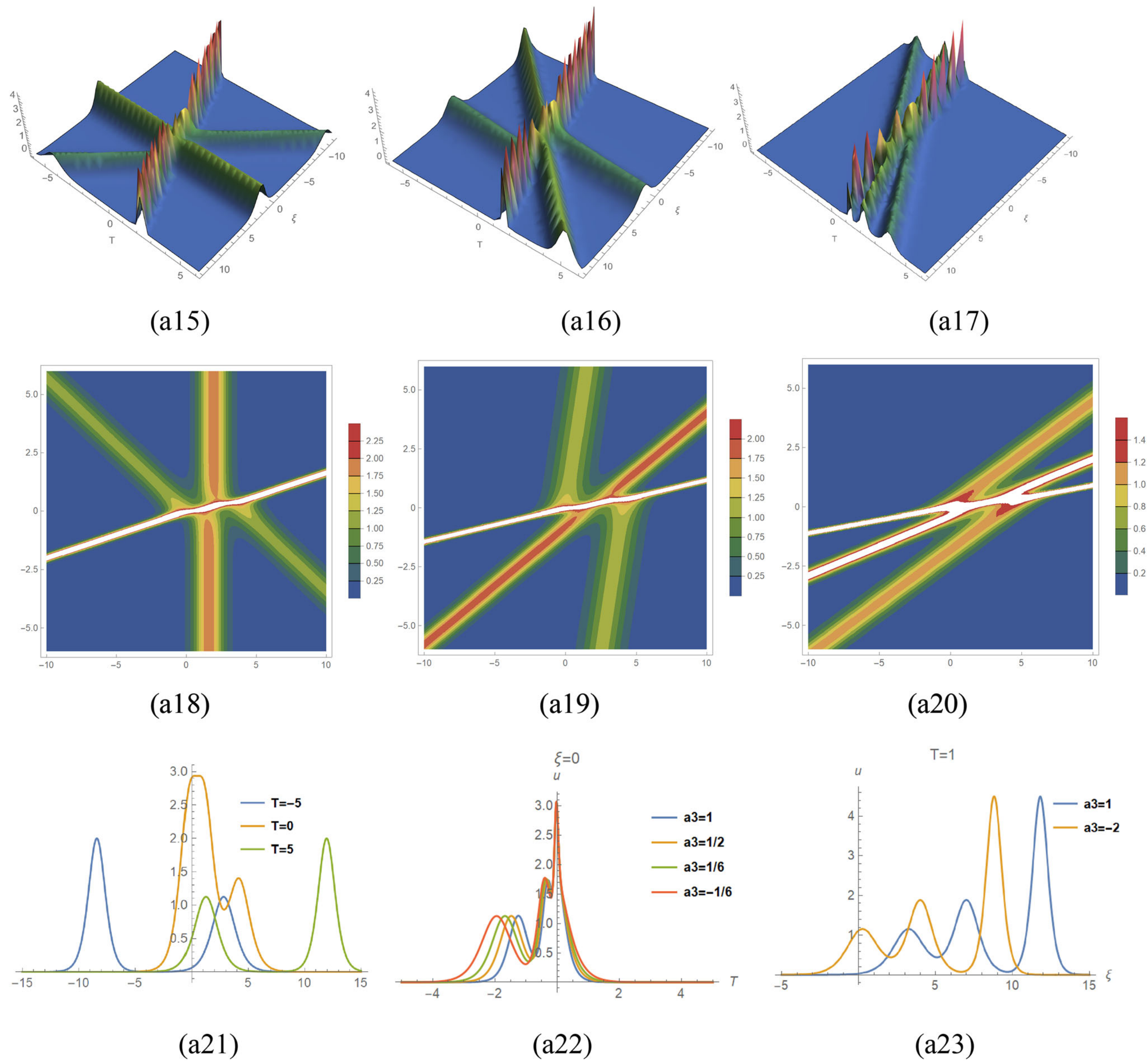

Fig. 3 Three-soliton solutions of Eq. (3). First row: 3D graphs of three-soliton solutions with $\lambda_1 = 2$, $\lambda_2 = 3$, $\lambda_3 = 3/2$, $a_2 = 1$, (a15) $a_3 = -4$;(a16) $a_3 = -2$;(a17) $a_3 = 1$. The second row is the corresponding contour plots. Third row: 2D graphs of three-soliton solutions

Substituting (34) (36) into (4), the one-breather wave solution is obtained:

$$u = 2\left(\frac{\lambda_1^2 e^{-\lambda_1(\xi - a_3 T)} + c_2\lambda_1^2 e^{\lambda_1(\xi - a_3 T)} - c_1\lambda_2^2\cos[\lambda_2(\xi - a_3 T)]}{e^{-\lambda_1(\xi - a_3 T)} + c_2 e^{\lambda_1(\xi - a_3 T)} + c_1\cos[\lambda_2(\xi - a_3 T)]}\right.$$
$$\left. - \frac{\left(-\lambda_1 e^{-\lambda_1(\xi - a_3 T)} + c_2\lambda_1 e^{\lambda_1(\xi - a_3 T)} - c_1\lambda_2\sin[\lambda_2(\xi - a_3 T)]\right)^2}{\left(e^{-\lambda_1(\xi - a_3 T)} + c_2 e^{\lambda_1(\xi - a_3 T)} + c_1\cos[\lambda_2(\xi - a_3 T)]\right)^2}\right) \quad (37)$$

In Fig. 4, by choosing proper parameters for Eq. (37), the dynamic diagrams of one-breather can be described: $\lambda_1 = \lambda_2 = 1/10$, $c_1 = -c_2 = 2$, (d1)$a_3 = 3$; (d2)$a_3 = 4$; (d3)$a_3 = 5$. From Figures (d1), (d2) and (d3), the same values of λ_1, λ_2, c_1, c_2 and a_2, along with a_3 increasing, the wave propagation direction changes clockwise and the period of the wave decreases. Figure (d4) is density plot of one-breather solution. From graph (d5), when $a_3 = 4$, as T increasing, the wave keeps the same shape and moves parallel to the right. From graph (d6), when $T = 3$, as the horizontal Coriolis parameter a_3 increasing, the wave keeps the same shape and moves parallel to the right.

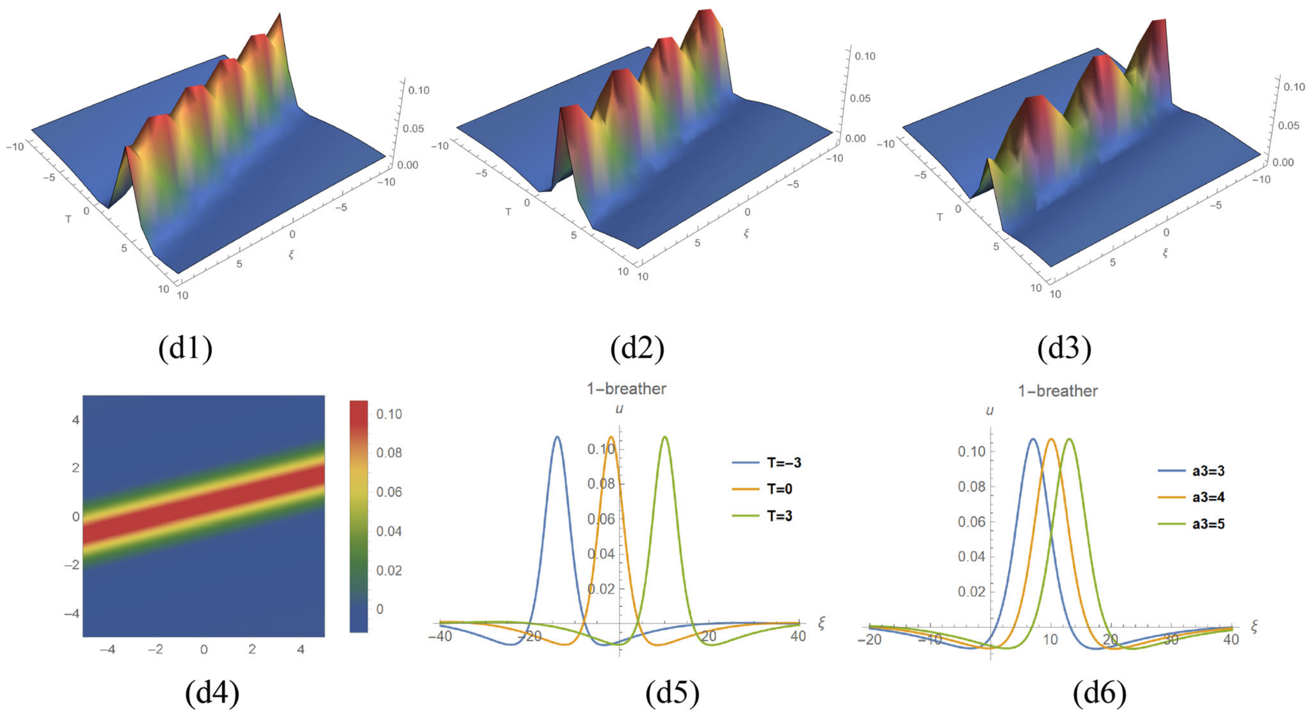

Fig. 4 One-breather of Eq. (3). The 3D graphs with $\lambda_1 = \lambda_2 = 1/10$, $c_1 = -c_2 = 2$, (d1)$a_3 = 3$;(d2)$a_3 = 4$;(d3)$a_3 = 5$. (d4) and (d5) are the density plots and the 2D graph with $a_3 = 4$; (d6) is the 2D graph with $T = 3$.

5 The interactions of one-soliton and one-breather

Supporting by the symbolic computation approach, the interactions of one-soliton and one-breather of Eq. (3) are gained, suppose:

$$f = \cosh\theta_1 + \cos\theta_2 + e^{\theta_3} + 1, \tag{38}$$

where $\theta_1 = \lambda_1(\xi - w_1 T)$, $\theta_2 = \lambda_1(\xi + w_2 T)$, $\theta_3 = \lambda_2(\xi + w_3 T)$, λ_1, w_1, λ_2, w_2, w_3 are real constant. Substituting (38) into (7) and setting the coefficients of $e^{\theta_3}\cos\theta_2$, $e^{\theta_3}\cosh\theta_1$, $\cos\theta_2\cosh\theta_1$, $e^{\theta_3}\sin\theta_2$, $e^{\theta_3}\sinh\theta_1$, $\sin\theta_2\sinh\theta_1$ equal to zero, this results in a group of six equations:

$$\begin{cases} -a_3\lambda_1^2 - w_2\lambda_1^2 + a_2\lambda_1^4 + a_3\lambda_3^2 + w_3\lambda_3^2 - 6a_2\lambda_1^2\lambda_3^2 + a_2\lambda_3^4 = 0, \\ a_3\lambda_1^2 - w_1\lambda_1^2 + a_2\lambda_1^4 + a_3\lambda_3^2 + w_3\lambda_3^2 + 6a_2\lambda_1^2\lambda_3^2 + a_2\lambda_3^4 = 0, \\ \lambda_1^2\left(w_1 + w_2 + 4a_2\lambda_1^2\right) = 0, \\ \lambda_1\lambda_3\left(2a_3 + w_2 + w_3 - 4a_2\lambda_1^2 + 4a_2\lambda_3^2\right) = 0, \\ \lambda_1\lambda_3\left(-2a_3 + w_1 - w_3 - 4a_2\lambda_1^2 + 4a_2\lambda_3^2\right) = 0, \\ \lambda_1^2(2a_3 - w_1 + w_2) = 0. \end{cases} \tag{39}$$

We select one of the solutions to continue analysis:

$$\begin{aligned} w_1 &= a_3 + a_2\lambda_1^2 + 3a_2\lambda_3^2, \\ w_2 &= \frac{-a_3\lambda_1^2 + a_2\lambda_1^4 - a_3\lambda_3^2 + w_1\lambda_3^2 - 10a_2\lambda_1^2\lambda_3^2 - 3a_2\lambda_3^4}{\lambda_1^2}, \\ w_3 &= -2a_3 + w_1 - 4a_2\lambda_1^2 - 4a_2\lambda_3^2. \end{aligned} \tag{40}$$

Substituting (38) (40) into (4), the interaction of one-soliton and one-breather is obtained:

$$\begin{aligned} u = 2\Bigg(&\frac{\lambda_3^2 e^{\lambda_3(\xi + w_3 T)} - \lambda_1^2\cos[\lambda_1(\xi + w_2 T)] + \lambda_1^2\cosh[\lambda_1(\xi - w_1 T)]}{1+e^{\lambda_3(\xi + w_3 T)} + \cos[\lambda_1(\xi + w_2 T)] + \cosh[\lambda_1(\xi - w_1 T)]} \\ &- \frac{(\lambda_3 e^{\lambda_3(\xi + w_3 T)} - \lambda_1\sin[\lambda_1(\xi + w_2 T)] + \lambda_1\sinh[\lambda_1(\xi - w_1 T)])^2}{(1+e^{\lambda_3(\xi + w_3 T)} + \cos[\lambda_1(\xi + w_2 T)] + \cosh[\lambda_1(\xi - w_1 T)])^2}\Bigg). \end{aligned} \tag{41}$$

where w_1, w_2, w_3 satisfy (40).

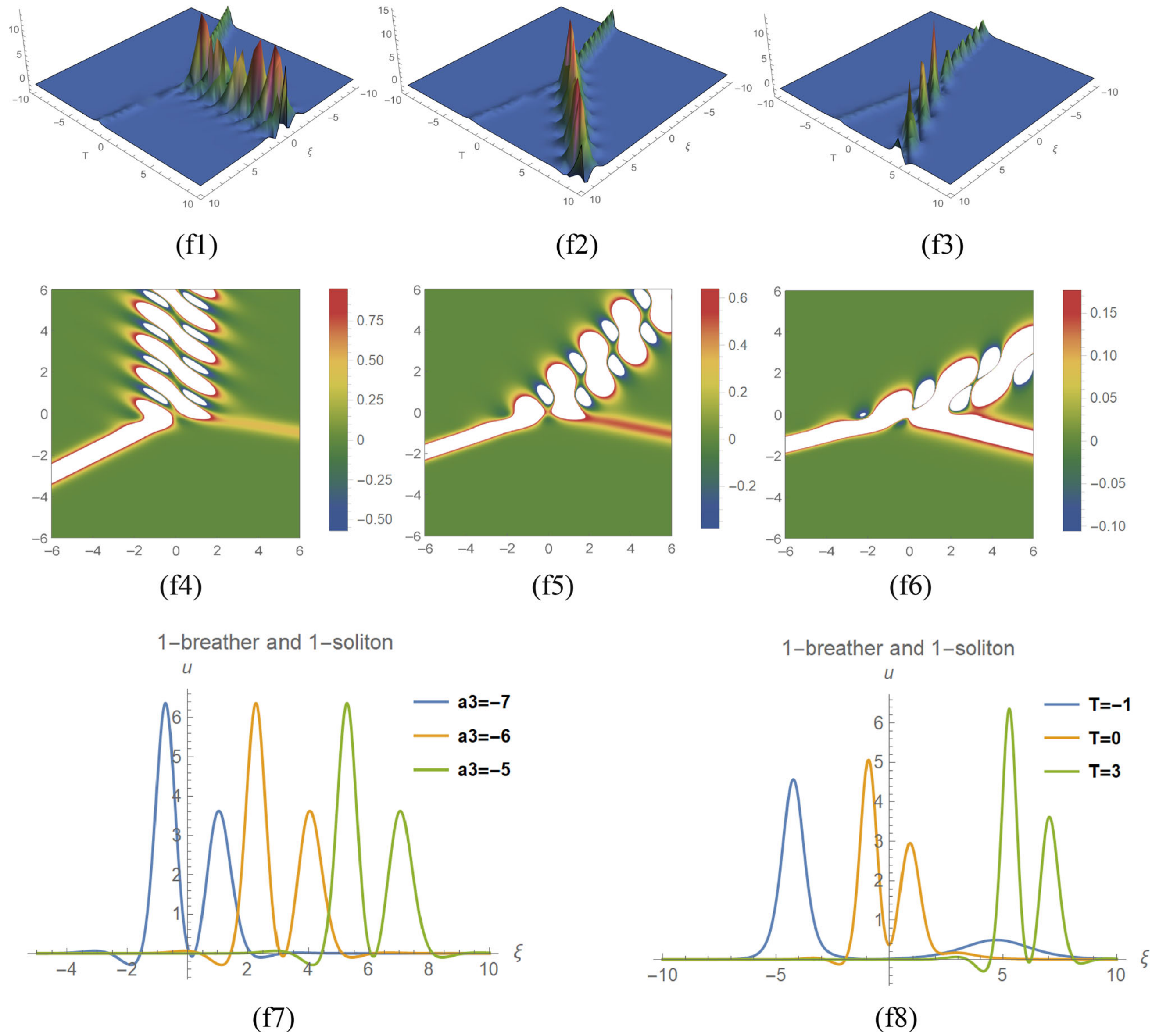

Fig. 5 The interaction solutions of one-soliton and one-breather of Eq. (3). 3D graphs with $\lambda_1 = 2$, $\lambda_3 = 1$, $a_2 = 1$, (f1) $a_3 = -7$;(f2)$a_3 = -6$;(f3)$a_3 = -5$. (f4) (f5) (f6) are density plots. (f7) (f8) are 2D plots.

In Fig. 5, by choosing proper parameters for (41), the dynamic diagrams of the interactions of one-soliton and one-breather can be described: $\lambda_1 = 2$, $\lambda_3 = 1$, $a_2 = 1$, (f1)$a_3 = -7$; (f2)$a_3 = -6$; (f3)$a_3 = -5$. From (f1)–(f3), the same values of λ_1, λ_3 and a_2, along with a_3 increasing, the wave propagation direction changes clockwise and the shape of both waves' changes. At same time, the angle between the two waves decreases, and the period decreases. The collision of two waves is inelastic, and they collide and merge into a wave, eventually forming a Y-type wave. From density Figures (f4) (f5) and (f6), we can clearly see the interaction of the two waves and notice that the moment of interaction of the two waves does not change with the changing of a_3. From 2D Figures (f7) and (f8), as a_3 increases, the waves keep the same shape and move parallel to the right; along T increasing, the shape and amplitude of wave changes.

6 The one-rogue wave solution

Supporting by the symbolic computation approach, the one-rogue wave solution of Eq. (3) is gained, suppose:

$$F = (d_1\xi + b_1 T + c_1)^2 + (d_2\xi + b_2 T + c_2)^2 + c_0,\ c_0 > 0. \tag{42}$$

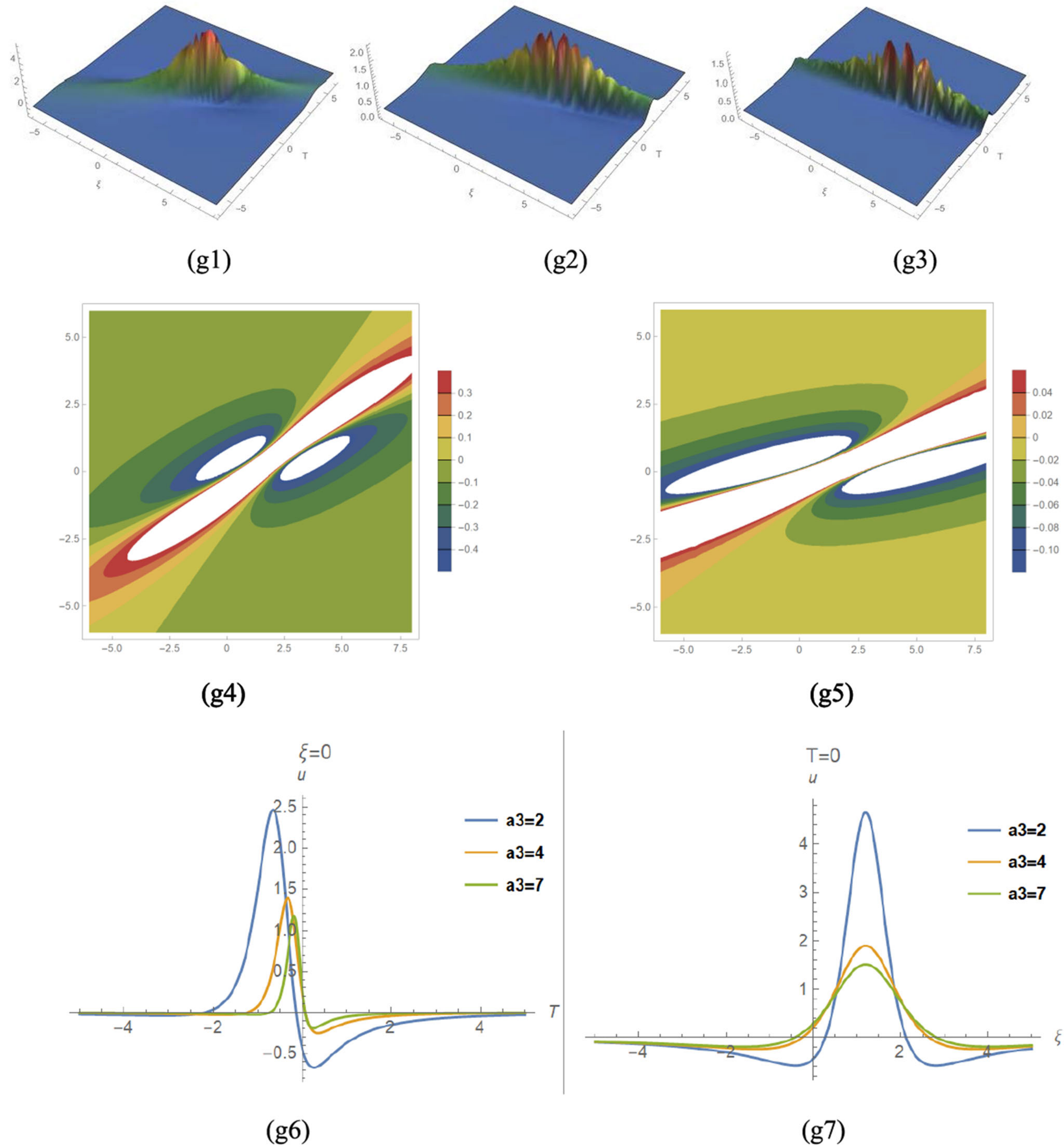

Fig. 6 One-rogue wave of Eq. (3). 3D graphs when $d_1 = 1$, $d_2 = 1/2$, $c_1 = -1$, $c_2 = -1$, $c_0 = 0$, $a_2 = 1/6$, (g1) $a_3 = 2$;(g2) $a_3 = 4$;(g3) $a_3 = 7$. Contour figures with $d_1 = 1$, $d_2 = 1/2$, $c_1 = -1$, $c_2 = -1$, $c_0 = 0$, $a_2 = 1/6$, (g4) $a_3 = 2$; (g5) $a_3 = 4$. g(6) g(7) are 2D graphs of the one-rogue wave.

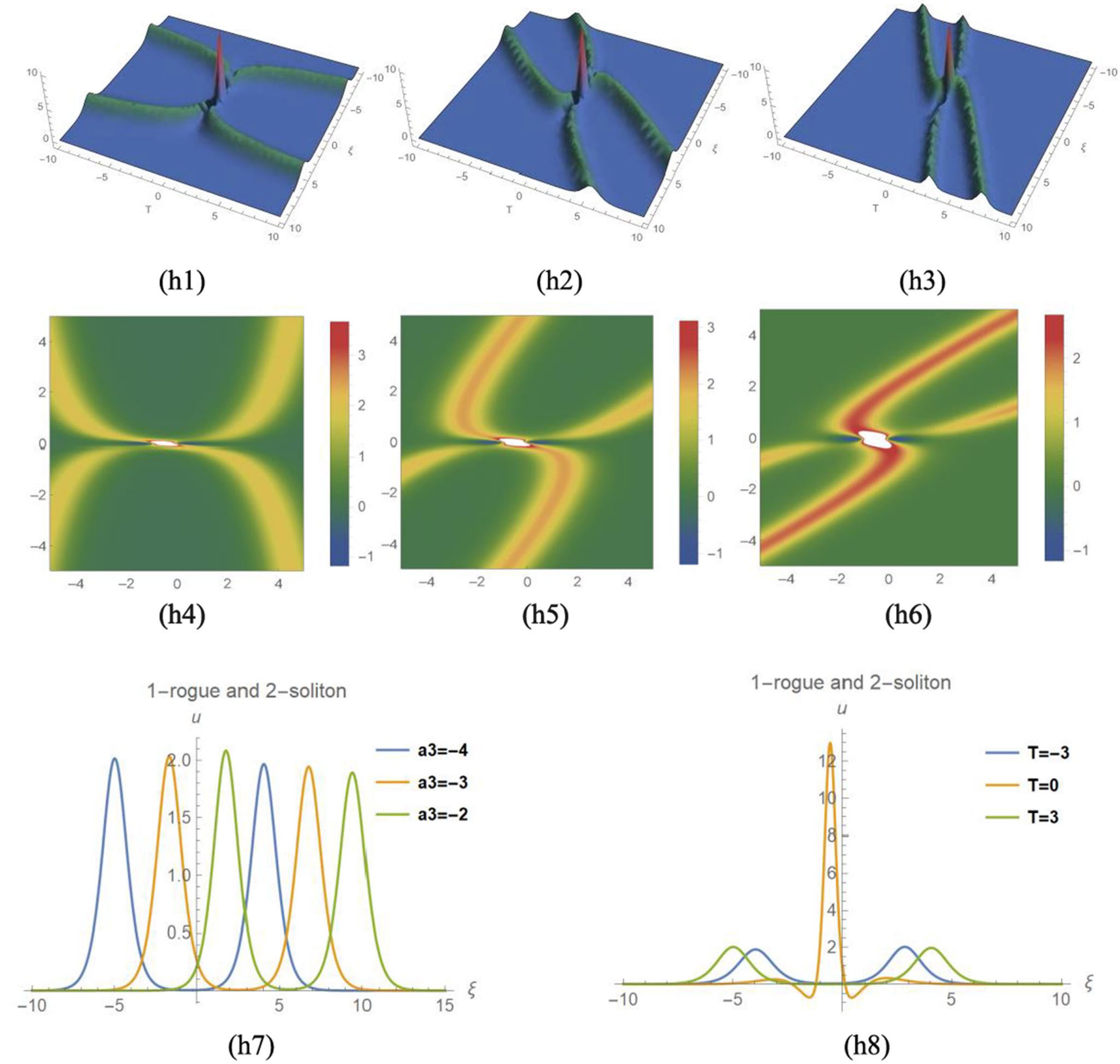

Fig. 7 Interaction solutions of two-soliton and one-rogue of Eq. (3). 3D graphs with $\lambda_1 = 1/2$, $\lambda_2 = \lambda_3 = 2$, $w_1 = 1$, $c_i = 1$, $(i = 1, 2, 3)$, $p = 1$, $a_2 = 1$(h1)$a_3 = -4$; (h2)$a_3 = -3$; (h3) $a_3 = -2$. (h4) (h5) (h6) are the corresponding density plots. (h7) (h8) are the 2D plots

where d_1, d_2, b_1, b_2, c_0, c_1, c_2 are real constant. Substituting (42) into (7), we assign coefficients T, T^2, ξ, ξ^2, ξT be equal to zero, and this results in a group of six equations:

$$\begin{cases} b_1\big(d_1(c_0 - c_1^2 + c_2^2) - 2c_1c_2d_2\big) + b_2\big(-2c_1c_2d_1 + d_2(c_0 + c_1^2 - c_2^2)\big) + a_3(d_1^2(c_0 - c_1^2 + c_2^2) \\ \quad - 4c_1c_2d_1d_2 + d_2^2(c_0 + c_1^2 - c_2^2)) + 6a_2(d_1^2 + d_2^2)^2 = 0, \\ \quad - 4\big(b_1^2(c_1d_1 + c_2d_2) + b_2\big(b_2c_1d_1 - a_3c_2d_1^2 + b_2c_2d_2 + 2a_3c_1d_1d_2 + a_3c_2d_2^2\big) \\ \quad + a_3b_1\big(2c_2d_1d_2 + c_1\big(d_1^2 - d_2^2\big)\big)\big) = 0, \\ \quad b_1^3d_1 + b_1b_2d_1(b_2 + 4a_3d_2) + b_1^2\big(b_2d_2 + a_3\big(d_1^2 - d_2^2\big)\big) + b_2^2\big(b_2d_2 + a_3\big(-d_1^2 + d_2^2\big)\big) = 0, \\ \quad (b_1c_1 + b_2c_2 + a_3c_1d_1 + a_3c_2d_2)\big(d_1^2 + d_2^2\big) = 0, \\ \quad \big(d_1^2 + d_2^2\big)\big(b_1^2 + a_3b_1d_1 + b_2(b_2 + a_3d_2)\big) = 0, \\ \quad \big(d_1^2 + d_2^2\big)\big(b_1d_1 + b_2d_2 + a_3\big(d_1^2 + d_2^2\big)\big) = 0. \end{cases} \tag{43}$$

We select one of the solutions to continue analysis:

$$
\begin{aligned}
b_1 &= -a_3 d_1, \\
b_2 &= \frac{1}{2}\left(-a_3 d_2 + \sqrt{-4b_1^2 - 4a_3 b_1 d_1 + a_3^2 d_2^2}\right), \\
c_0 &= \frac{-6a_2(d_1^2 + d_2^2)^2 + 2a_3 c_1 c_2 d_1 d_2 - a_3 c_1^2 d_2^2 + a_3 c_2^2 d_2^2}{a_3 d_2^2}.
\end{aligned} \tag{44}
$$

Substituting (42) (44) into (4), the one-rogue wave is conducted:

$$
u = 4\left(-\frac{2(d_1 A + d_2 B)^2}{\Theta^2} + \frac{d_1^2 + d_2^2}{\Theta}\right). \tag{45}
$$

$$
\begin{aligned}
\Theta &= c_0 + A^2 + B^2, \\
A &= c_1 - a_3 d_1 T + d_1 \xi, \\
B &= c_2 + d_2 \xi.
\end{aligned}
$$

In Fig. 6, by choosing proper parameters for (45), the dynamic diagrams of one-rogue wave can be described: $d_1 = 1$, $d_2 = 1/2$, $c_1 = -1$, $c_2 = -1$, $c_0 = 0$, $a_2 = 1/6$, (g1) $a_3 = 2$;(g2)$a_3 = 4$;(g3) $a_3 = 7$. From (g1)—(g3), the same values of d_1, d_2, c_1, c_2, c_0 and a_2, along with a_3 changing, the wave propagation direction changes clockwise. From (g4) and (g5), different values of a_3 lead to a big change of density. From (g6), (g7), when $\xi = 0$ and $T = 0$, along with a_3 increasing, amplitudes decrease and shapes change.

7 The interactions of two-soliton and one-rogue

Supporting by the symbolic computation approach, the interaction of two-soliton and one-rogue of Eq. (3) is obtained, suppose:

$$
f = \theta_1^2 + \theta_2^2 + \mathrm{e}^{p\theta_3} + \mathrm{e}^{-p\theta_3}, \tag{46}
$$

where $\theta_i = \lambda_i \xi + w_i T + c_i$, $(i = 1, 2, 3)$, λ_i, w_i are real constant.

Putting (46) in (7) and setting the coefficients of $\mathrm{e}^{-p\theta_3}$, $\mathrm{e}^{p\theta_3}$, T, T^2, $T\xi$, ξ, ξ^2 and the coefficients of the cross terms be equal to zero, this results in a group of eighteen equations, we select one of the solutions to continue analysis:

$$
\begin{aligned}
w_1 &= \frac{-a_3\lambda_1^2 - w_2\lambda_2 - a_3\lambda_2^2}{\lambda_1}, \\
w_2 &= -a_3\lambda_3 - a_2 p^2 \lambda_3^2.
\end{aligned} \tag{47}
$$

Substituting (46) (47) into (4), the interaction of two-soliton and onebreather is gained:

$$
\begin{aligned}
u = 2\Bigg(&\frac{2\lambda_1^2 + 2\lambda_2^2 + p^2\lambda_3^2 \mathrm{e}^{-p(\lambda_3\xi + w_3 T + c_3)} + p^2\lambda_3^2 \mathrm{e}^{p(\lambda_3\xi + w_3 T + c_3)}}{\mathrm{e}^{-p(\lambda_3\xi + w_3 T + c_3)} + \mathrm{e}^{p(\lambda_3\xi + w_3 T + c_3)} + (\lambda_1\xi + w_1 T + c_1)^2 + (\lambda_2\xi + w_2 T + c_2)^2} \\
&- \frac{(-p\lambda_3 \mathrm{e}^{-p(\lambda_3\xi + w_3 T + c_3)} + p\lambda_3 \mathrm{e}^{p(\lambda_3\xi + w_3 T + c_3)} + 2\lambda_1(\lambda_1\xi + w_1 T + c_1) + 2\lambda_2(\lambda_2\xi + w_2 T + c_2))^2}{(\mathrm{e}^{-p(\lambda_3\xi + w_3 T + c_3)} + \mathrm{e}^{p(\lambda_3\xi + w_3 T + c_3)} + (\lambda_1\xi + w_1 T + c_1)^2 + (\lambda_2\xi + w_2 T + c_2)^2)^2}\Bigg).
\end{aligned} \tag{48}
$$

where w_1, w_2 satisfy (47).

In Fig. 7, by choosing proper parameters for (48), the dynamic diagrams of the interaction of two-soliton and one-rogue can be described: $\lambda_1 = 1/2$, $\lambda_2 = \lambda_3 = 2$, $w_1 = 1$, $c_i = 1$, $(i = 1, 2, 3)$, $p = 1$, $a_2 = 1$, (h1) $a_3 = -4$; (h2) $a_3 = -3$; (h3)$a_3 = -2$. From (h1), (h2) and (h3), the same values of λ_1, λ_2, λ_3, w_1, c_i and a_2, along with a_3 increasing, the wave propagation direction changes clockwise and the shape of both waves' changes. At same time, the angle between the two solitons decreases. We can see that the two solutions are bright solitons, and the collisions are elastic. Their speeds and shapes keep no change after collision; two solitons have phase shifts after the interactions, and as a_3 changes, the position of the interaction between solitons does not change, and one-rogue wave is always at the center of the collision. From density Figures (h4) (h5) and (h6), we can clearly see the interaction of the two waves and notice that the moment of interaction of the two waves does not change with the changing of a_3. From 2D Figures (h7) and (h8), as a_3 increases, the waves move parallel to the right, along T increasing, the shape and amplitude of wave change the one-rogue wave in the center position of the two solitons.

8 Conclusions

This manuscript investigates the wave–wave interaction of the extended KdV equation with complete Coriolis parameters. Mainly apply Hirota bilinear method, and with the assistance of small parameter perturbation, N-soliton solution is represented. Application of the symbolic computation approach, one-breather, one-rogue wave and interaction between one-soliton and one-breather, interaction between two-soliton and one-rogue solutions are obtained. These solutions are new solutions, which are helpful to understand diverse physical phenomena in the atmosphere and ocean.

The effect of the horizontal Coriolis parameters a_3 on propagation direction, period, and shape of wave is revealed. From all figures, it can be found that the change of Coriolis parameter a_3 affects the propagation direction of the wave, and the wave rotates clockwise with the Coriolis parameter a_3 increasing. If it is a periodic wave, an increase in a_3 will also decrease the period. Figure 5 shows the inelastic collision of one-soliton and one-breather, which eventually form a Y-type wave. Figure 7 shows the elastic collision of two solitons, and one-rogue wave is always at the center of the collision. From Fig. 2, 3, 5, 7, the moment of interaction of the waves does not change with the change of a_3.

Acknowledgements Our article is supported by the National Natural Science Foundation of China (12262025). The Natural Science Foundation of Inner Mongolia Autonomous Region (2022QN01003). The Program for Young Talents of Science and Technology in Universities of Inner Mongolia Autonomous Region (NJYT23099 and NMGIRT2208). Inner Mongolia Autonomous Region University research Project (NJZY23116). The Program for improving the Scientific Research Ability of Youth Teachers of Inner Mongolia Agricultural University (BR220126). Basic scientific research funds of universities directly under the Inner Mongolia Autonomous Region (22BR0902).

Declarations

Conflict of interest We declare that we have no financial and personal relationships with other people or other organizations that can inappropriately influence our work.

Data Availability Statement Data availability is not applicable to this article as no new data were created or analyzed in this study.

References

1. R. Zhang, L. Yang, Theoretical analysis of equatorial near-inertial solitary waves under complete Coriolis parameters. Acta. Oceanol. Sin. **40**, 54 (2021)
2. R.H. Pletcher, J.C. Tannehill, D.A. Anderson, Computational fluid mechanics and heat transfer (CRC press, 2012)
3. P. Muggli, S.F. Martins, J. Vieira et al., Interaction of ultra relativistic e- e+ fireball beam with plasma. New. J. Phys. **22**, 013030 (2020)
4. P.F. Han, T. Bao, Hybrid localized wave solutions for a generalized Calogero–Bogoyavlenskii–Konopelchenko–Schiff system in a fluid or plasma. Nonlinear Dyn. **108**, 2513 (2022)
5. Y.Y. Li, H.X. Jia, D.W. Zuo, Multi-soliton solutions and interaction for a (2+1)-dimensional nonlinear Schrödinger equation. Optik **241**, 167019 (2021)
6. B. Kaltenbacher, Mathematics of nonlinear acoustics. Evol. Equ. Control. The. **4**, 447 (2015)
7. J. Luo, Q. Zhou, T. Jin, Numerical simulation of nonlinear phenomena in a standing-wave thermoacoustic engine with gas-liquid coupling oscillation. Appl Therm. Eng. **207**, 118131 (2022)
8. X.M. Tan Zhaqilao, Three wave mixing effect in the (2+1)-dimensional Ito equation. Int. J. Comput. Math. **98**, 1921 (2021)
9. D. Zhao Zhaqilao, The abundant mixed solutions of (2+1)-dimensional potential Yu–Toda–Sasa–Fukuyama equation. Nonlinear Dyn. **103**, 1055 (2021)
10. Y.F. Yue, Y. Chen, Dynamics of localized waves in a (3 + 1)-dimensional nonlinear evolution equation. Mod. Phys. Lett. B. **33**, 1950101 (2019)
11. Y. Shen, B. Tian, T.Y. Zhou, In nonlinear optics, fluid dynamics and plasma physics: symbolic computation on a (2+1)-dimensional extended Calogero–Bogoyavlenskii–Schiff system. Eur. Phys. J. Plus. **136**, 5 (2021)
12. Y. Shen, B. Tian S.H. Liu, T.Y. Zhou, Studies on certain bilinear form, N-soliton, higher-order breather, periodic-wave and hybrid solutions to a (3+ 1)-dimensional shallow water wave equation with time-dependent coefficients. Nonlinear Dyn. **108**, 2447 (2022)
13. L.L. Huang, Y.F. Yue, Y. Chen, Localized waves and interaction solutions to a (3+1)-dimensional generalized KP equation. Comput. Math. Appl. **76**, 831 (2018)
14. Y.F. Yue, L.L. Huang, Y. Chen, N-solitons, breathers, lumps and rogue wave solutions to a (3+1)-dimensional nonlinear evolution equation. Comput. Math. Appl. **75**, 2538 (2018)
15. Y.Y. Feng, Sudao Bilige, Multi-breather, multi-lump and hybrid solutions to a novel KP-like equation. Nonlinear Dyn. **106**, 879 (2021)
16. D. Zhao, Zhaqilao, Three-wave interactions in a more general (2+1)-dimensional Boussinesq equation. Eur. Phys. J. Plus. **135**, 617 (2020)
17. A. Yusuf, T.A. Sulaiman, M. Inc, M. Bayram, Breather wave, lump-periodic solutions and some other interaction phenomena to the caudrey–dodd–gibbon equation. Eur. Phys. J. Plus. **135**, 7 (2020)
18. J.G. Liu, W.H. Zhu, L. Zhou, Multi-wave, breather wave, and interaction solutions of the Hirota–Satsuma–Ito equation. Eur. Phys. J. Plus. **135**, 1 (2020)
19. X. Zhao, B. Tian, X.X. Du, C.C. Hu, S.H. Liu, Bilinear bcklund transformation, kink and breather-wave solutions for a generalized (2+1)-dimensional hirota–satsuma–ito equation in fluid mechanics. Eur. Phys. J. Plus. **136**, 2 (2021)
20. Z. Zhao, J. Yue, L. He, New type of multiple lump and rogue wave solutions of the (2+1)-dimensional Bogoyavlenskii–Kadomtsev–Petviashvili equation. Appl. Math. Lett. **133**, 108294 (2022)
21. J.G. Liu, W.H. Zhu, Y. He, Variable-coefficient symbolic computation approach for finding multiple rogue wave solutions of nonlinear system with variable coefficients. Z. Angew. Math. Phys. **72**, 1 (2021)
22. P.Y. Alexis, G.R. Kol, Breather solitons and rogue waves supported by thermally induced self-trapping in a one-dimensional microcavity system. Eur. Phys. J. Plus. **137**, 670 (2022)

23. X.M. Wang, P.F. Li, Breathers and solitons for the coupled nonlinear Schrödinger system in three-spine α-helical protein. Chin. Phys. B. **30**, 100509 (2021)
24. Zhaqilao, A symbolic computation approach to constructing rogue waves with a controllable center in the nonlinear systems. Comput. Math. Appl. **75**, 3331 (2018)
25. H. Hu, X. Li, Nonlocal symmetry and interaction solutions for the new (3+1)-dimensional integrable Boussinesq equation. Math. Model. Nat. Pheno. **17**, 10 (2022)
26. Y. Shen, Y. Yang, Bäcklund transformation and exact solutions to a generalized (3+1)-dimensional nonlinear evolution equation. Discrete Dyn. Nat. Soc. **2022**, 5598381 (2022)
27. J.W. Wu, Y.J. Cai, J. Lin, Residual symmetries, consistent-Riccati-expansion integrability, and interaction solutions of a new (3+ 1)-dimensional generalized Kadomtsev–Petviashvili equation. Chin. Phys. B. **31**, 030201 (2022)
28. N. Cao, X.J. Yin, S.T. Bai, L.Y. Xu, Breather wave, lump type and interaction solutions for a high dimensional evolution model. Chaos Solitons Fract. **172**, 113505 (2023)
29. N. Cao, X.J. Yin, S.T. Bai, L.Y. Xu, A governing equation of Rossby waves and its dynamics evolution by Bilinear neural network method. Phys. Scripta. **98**, 065222 (2023)
30. D. Zhao Zhaqilao, on two new types of modified short pulse equation. Nonlinear Dyn. **100**, 615 (2020)
31. L. Kaur, A.M. Wazwaz, Lump, breather and solitary wave solutions to new reduced form of the generalized BKP equation. Int. J. Numer. Method H. **29**, 569 (2018)
32. K.H. Yin, X.P. Cheng, J. Lin, Soliton molecule and breather-soliton molecule structures for a general sixth-order nonlinear equation. Chin. Phys. Lett. **38**, 080201 (2021)
33. M.H. Huang, One-, two- and three-soliton, periodic and cross-kink solutions to the (2+1)-D variable-coefficient KP equation. Mod. Phys. Lett. B. **34**, 2050045 (2020)
34. P.F. Han, Taogetusang, Lump-type, breather and interaction solutions to the (3+1)-dimensional generalized KdV-type equation. Mod. Phys. Lett. B. **34**, 2050329 (2020)
35. X. Lü, S.J. Chen, Interaction solutions to nonlinear partial differential equations via Hirota bilinear forms: one-lump-multi-stripe and one-lump-multi-soliton types. Nonlinear Dyn. **103**, 947 (2021)
36. M.J. Ablowitz, P.A. Clarkson, *Solitons* (Cambridge University Press, Cambridge, Nonlinear Evolution Equations and Inverse Scattering, 1991)
37. G.X. Wang, X.B. Wang, B. Han, Inverse scattering of nonlocal Sasa-Satsuma equations and their multi soliton solutions. Eur. Phys. J. Plus. **137**, 3 (2022)
38. Y. Li, S.F. Tian, Inverse scattering transform and soliton solutions of an integrable nonlocal Hirota equation. Commun. Pur. Appl. Anal. **21**, 293 (2022)
39. H. Ma, S. Yue, A. Deng, D'Alembert wave, the Hirota conditions and soliton molecule of a new generalized KdV equation. J. Geom. Phys. **172**, 104413 (2022)
40. S. Arshed, N. Raza, A.R. Butt et al., Multiple rational rogue waves for higher dimensional nonlinear evolution equations via symbolic computation approach. J. Ocean. Eng. Sci. **8**(1), 33 (2021)
41. T.A. Mesquita, Symbolic approach to 2-orthogonal polynomial solutions of a third order differential equation. Math. Comput. Sci. **16**(1), 6 (2022)
42. H. Jafari, N. Kadkhoda, D. Baleanu, Fractional lie group method of the time-fractional boussinesq equation. Nonlinear Dyn. **81**(3), 1569 (2015)
43. V. Jadaun, Soliton solutions of a (3+1)-dimensional nonlinear evolution equation for modeling the dynamics of ocean waves. Phys. Scr. **96**, 095204 (2021)
44. M.B. Abd-El-Malek, A.M. Amin, New exact solutions for solving the initial-value-problem of the KdV–KP equation via the Lie group method. Appl. Math. Comput. **261**, 408 (2015)
45. X. Wang, C. Liu, L. Wang, Darboux transformation and rogue wave solutions for the variable-coefficients coupled Hirota equations. J. Math. Anal. Appl. **449**, 1534 (2017)
46. B.Q. Li, Y.L. Ma, Extended generalized darboux transformation to hybrid rogue wave and breather solutions for a nonlinear Schrödinger equation. Appl. Math. Comput. **386**, 125469 (2020)
47. D.Y. Yang, B. Tian, M. Wang et al., Lax pair, Darboux transformation, breathers and rogue waves of an N-coupled nonautonomous nonlinear Schrödinger system for an optical fiber or a plasma. Nonlinear Dyn. **107**, 2657 (2022)
48. X.J. He, X. Lü, M.G. Li, Bäcklund transformation, Pfaffian, Wronskian and Grammian solutions to the (3+1)-dimensional generalized Kadomtsev-Petviashvili equation. Anal. Math. Phys. **11**, 1 (2021)
49. S.J. Chen, X. Lü, W.X. Ma, Bäcklund transformation, exact solutions and interaction behaviour of the (3+1)-dimensional Hirota-Satsuma-Ito-like equation. Commun. Nonlinear. Sci. **83**, 105135 (2020)
50. L. Biao, Y. Chen, H.Q. Zhang, Auto- Bäcklund transformation and exact solutions for compound KdV-type and compound KdV–Burgers-type equations with nonlinear terms of any order. Phys. Lett. A. **305**, 377 (2002)
51. Zhaqilao, Rogue waves and rational solutions of a (3+1)-dimensional nonlinear evolution equation. Phys. Lett. A. **377**, 3021 (2013)